

Multi-Stage Monte Carlo Tree Search for Non-Monotone Object Rearrangement Planning in Narrow Confined Environments

Hanwen Ren and Ahmed H. Qureshi

Abstract—Non-monotone object rearrangement planning in confined spaces such as cabinets and shelves is a widely occurring but challenging problem in robotics. Both the robot motion and the available regions for object relocation are highly constrained because of the limited space. This work proposes a Multi-Stage Monte Carlo Tree Search (MS-MCTS) method to solve non-monotone object rearrangement planning problems in confined spaces. Our approach decouples the complex problem into simpler subproblems using an object stage topology. A subgoal-focused tree expansion algorithm that jointly considers the high-level planning and the low-level robot motion is designed to reduce the search space and better guide the search process. By fitting the task into the MCTS paradigm, our method produces optimistic solutions by balancing exploration and exploitation. The experiments demonstrate that our method outperforms the existing methods in terms of the planning time, the number of steps, and the total move distance. Moreover, we deploy our MS-MCTS to a real-world robot system and verify its performance in different scenarios.

I. INTRODUCTION

Object rearrangement planning in narrow, confined spaces such as cabinets, shelves, and fridges is essential for robots working in such environments. For example, robots must rearrange objects by grouping the same type for maintenance needs and create particular patterns to use the confined space better. Object rearrangement planning is generally known as NP-hard [1] because the planner needs to figure out the moving order of the objects and the intermediate relocation regions. This problem can further be categorized as follows based on the moving count of objects and robot actions. The monotone instances, where each object can be relocated at most once, and the non-monotone instances, where they can be relocated multiple times in the scene. Regarding robot movements, the prehensile instances consider robot pick-and-place actions, whereas non-prehensile instances use push actions.

This work focuses on prehensile non-monotone object arrangement planning problems in narrow, confined spaces. The confined setting introduces an extra constraint on the robot's motion compared to tabletop environments. In tabletop environments, robots can grasp objects from the top and use the space above the objects to avoid collisions during relocation. However, in confined environments with a covered top and a side opening, the objects can only be accessed from the side. Hence, robots always occupy

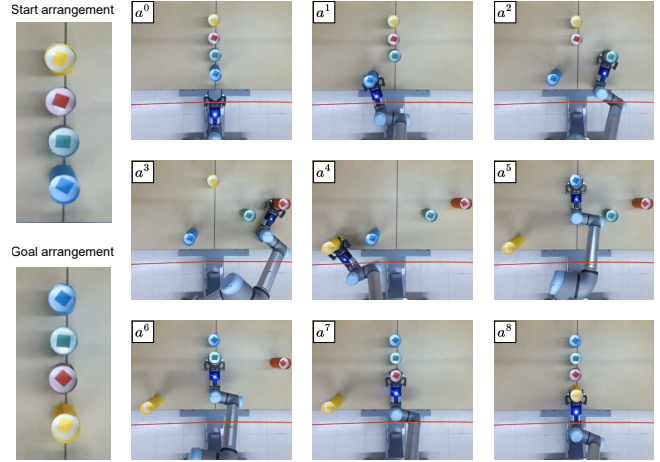


Fig. 1: A four objects flipping case solved by our method in 8 steps, whereas another state-of-the-art method takes 23 steps on average.

a certain amount of space during the motion, resulting in fewer regions for objects to be placed and a high chance of object-to-object and object-to-robot collisions.

Most existing works solve the non-monotone rearrangement planning problem using diverse tree search variations. The general method treats the start arrangement as the root, and the tree keeps growing until the goal arrangement is achieved. The parent and child tree nodes are linked with a single object movement, i.e., an object is relocated to another region by the robot in a collision-free manner. Once the goal arrangement is found, the algorithm backtracks and recovers the entire plan. Due to the elevated complexity of the non-monotone cases, intelligent search algorithms are developed to solve them in a reasonable time budget [2]. However, most of these approaches only aim to find a feasible solution, while the quality of the result, such as the number of steps and distance traveled by the robot, are not optimized.

Therefore, in this paper, we propose an efficient Multi-Stage Monte Carlo Tree Search (MS-MCTS) approach that solves prehensile non-monotone object rearrangement planning problems in narrow, confined spaces with a higher success rate and fewer steps and less distance traveled than any existing methods. We also deploy the method to real-world scenarios and verify its sim-to-real generalization abilities. In summary, the main contributions of the proposed work are listed as follows:

- A non-monotone object rearrangement planner that

Hanwen Ren and Ahmed H. Qureshi are with the Department of Computer Science, Purdue University, West Lafayette, IN, USA, 47907. Email {ren221, ahqureshi}@purdue.edu

finds high-quality solutions by fitting the problem into the MCTS paradigm. Our method suits real-world robotics systems of different configurations.

- A specially designed subgoal-focused tree expansion algorithm that jointly considers the high-level relocation planning and low-level robot motion planning, which constrains the search within a limited sub-space.
- A novel object relocation order heuristic helps the planner decouple the complicated problem into simpler sub-problems, which is proven suitable for the narrow, confined spaces setting.
- A computationally efficient robot motion planner that minimizes the swept volume of the robot actions.

II. RELATED WORK

Object rearrangement planning in various environments is an active and widely researched problem in robotics, which is also a frequently occurring instance in the field of Navigation Among Movable Obstacles (NAMO) [3], [4] and Task And Motion Planning (TAMP) [5], [6]. Since it needs to consider both the high-level task planner and the low-level motion planner in environments with movable objects, the problem is generally considered NP-hard. Existing works solve the rearrangement planning problem under different settings. [7]–[9] solves monotone instances by checking all the permutations of the object relocation order in a reverse-time manner. [10]–[15] perform the planning on tabletop environments utilizing tree search with modified growing strategies or search hierarchy followed by backtracking. Others [16]–[20] put the recent advancement of the deep neural network into play and let the planning agent learn the underlying logic of various moves using the collected dataset. Aside from the open workspace, [2], [21]–[23] assume more constrained environments like the cabinets or other confined spaces with only one opening in the front, which are more common in real-world scenarios. Their strategies include performing intelligent expansions or pre-pruning the search trees so that invalid actions can be filtered out at early stages. These moves shrink the search space and increase efficiency. Compared with our method that finds an optimistic solution, most of them only aim to find a valid solution in a depth-first search manner without considering the quality of the resulting plans.

In order to find high-quality optimistic solutions, the Monte Carlo Tree Search (MCTS) [24] has recently been applied to the rearrangement planning problems. MCTS has been proven extremely useful in balancing the exploration and exploitation during the search process, resulting in strong performances. The AlphaGo, AlphaZero [25]–[27] took advantage of MCTS and beat the top-ranked human go player in 2016. In rearrangement planning problems, [28] use MCTS to achieve both efficiency and scalability in tabletop environments. [29], [30] fit the non-prehensile object rearranging and sorting tasks into the MCTS paradigm to achieve decent performance. Different from these works, we use the MCTS in the confined spaces setting with specially designed algorithms to guide the expansion and simulation

process, resulting in improved performances in the runtime and the plan quality.

III. PROBLEM FORMULATION

Let a confined workspace with one narrow opening at the front be denoted as $\mathcal{W} \subset \mathbb{R}^3$. In this confined space, $n \in \mathbb{N}$ identical but uniquely labeled cylindrical objects, with radius b , are denoted as $\mathcal{O} = \{o_1, \dots, o_n\}$. The ground surface of the workspace has many placement location candidates $p \in \mathcal{P} \subset \mathbb{R}^2$ where the geometric center of the objects' bottom surface can be placed. The placement locations associated with all objects at step t form the object arrangement $a^t = \{p_1^t, \dots, p_n^t\} \subset \mathcal{A}$, where \mathcal{A} is the arrangement space. The $a^t[o_i] = p_i^t$ denotes that object o_i locates at region p_i^t in arrangement a^t . A robot arm \mathcal{M} equipped with a gripper is placed in front of the workspace opening at location p_m to perform prehensile object relocation actions. One relocation action $r^t = (r_{pick}^t, r_{place}^t)$ at step t involves both picking a certain object at its current region and placing it at the next region, resulting in a new object arrangement a^{t+1} . While performing such actions, the robot follows a certain manipulation path $\pi(r^t) = \{q_0^t, \dots, q_k^t\}$, where each $q_i \in \mathcal{Q} \subset \mathbb{R}^d$ is an instance in the d -dimensional arm configuration space. The volume occupied by the robot arm during a relocation action is represented as $V(\pi(r^t))$. A relocation action involving object o_k at step t is valid if it satisfies the collision constraint, written as $V(\pi(r^t)) \cap V(a^t \setminus a^t[o_k]) = \emptyset$, where the term, $V(a^t \setminus a^t[o_k])$, is the space occupied by all other objects except the one that is currently being relocated.

Using the notations above, the non-monotone object rearrangement planning problem is formally defined as follows. Given n -objects start arrangement a^s and goal arrangement a^g , find a sequence of valid and optimistic robot actions $R = \{(r_{pick}^0, r_{place}^0), (r_{pick}^1, r_{place}^1), \dots\}$ that relocates all objects from their start to the goal placements.

IV. METHODOLOGY

This section formally introduces the proposed Multi-Stage Monte-Carlo Tree Search (MS-MCTS) object rearrangement planner and the related modules in detail.

A. Linear Motion Planner

We design a Linear Motion Planner (LMP) to move the gripper toward the objects and perform prehensile actions. In the confined spaces setting, where the robot cannot use the space on the upper Z axis to perform grasp action and avoid collisions, the linear planner minimizes the swept volume by first aiming the gripper toward the objects and then moving it linearly in the XY plane while maintaining a fixed height on the Z axis. The robot configurations for linear movement $\pi(r^t)$ can be obtained by calculating the Inverse Kinematics (IK) [31] on the discretized points along the path. To relocate an object o_i from its current region p_i^t to the next region p_i^{t+1} , the gripper first moves from its home location p_m to p_i^t , picks the object up, and retrieve it back. Then it goes to p_i^{t+1} , places the object, and returns to

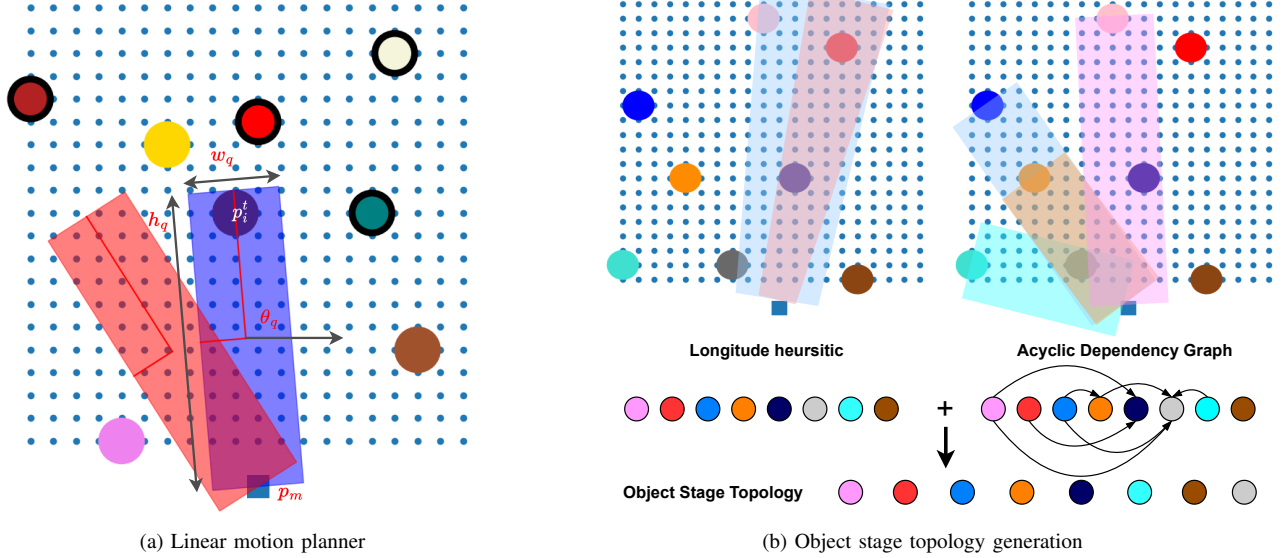


Fig. 2: (a) The gripper at p_m uses the collision-free picking tunnel (blue) and placing tunnel (red) generated from our linear motion planner to relocate the object at p_i^t . Objects with a black contour are already placed at their goal regions. (b) The left sub-figure shows the order from the longitude heuristic while the right one illustrates the generation process of the dependency graph. For example, the goal region of the grey object blocks the turquoise, blue, orange, and pink objects, which creates four edges toward the grey object in the dependency graph. The final object stage topology is created by jointly considering the longitude heuristic and the dependency graph.

p_m . In order to check collisions, the robot's swept volume $V(\pi(r^t))$ during the linear movement is constructed by a rectangular tunnel with length h_q , width w_q , tilted at angle θ_q shown in Fig. 2 (a). In the rest of the paper, we use the terms picking tunnel and placing tunnel to denote the swept volume of the robot's prehensile actions. The tunnel parameters h_q and θ_q that moves the gripper from p_m to an object with radius b located at p_i^t can be calculated by $h_q = \|p_i^t - p_m\|_2 + b$, $\theta_q = \arccos\left(\frac{i \cdot (p_i^t - p_m)}{\|p_i^t - p_m\|_2}\right)$, where i is the unit vector on the positive X axis. The parameter w_q is the robot's maximum width when the gripper moves linearly. There are three advantages of our linear motion planner. First, it is a general method that suits all robots of various configurations. Second, the collision between the objects and the robot motion tunnel can be efficiently checked by the Separating Axis Theorem [32]. Third, the linear motion planner minimizes the swept volume, resulting in a higher probability of finding valid solutions.

B. Object Stage Topology Generation

We create an object stage topology that defines the optimal order to place all objects in their goal regions, which considers the longitude heuristic and dependency graph of goal arrangement jointly. The longitude heuristic prioritizes objects that are to be placed farther behind than closer to the robot. Recall the linear motion planner introduced above. The objects placed at their goal regions in the front side of the environment are more likely to block the placing tunnels for objects further back as shown in the left image of Fig. 2 (b). This implies that objects with front-end goals

must be relocated to an additional buffer region before returning, wasting the steps of getting them to the goal regions in the first place. Thus, it is more appropriate to relocate objects in the decreasing order of their longitudinal distances between their goals and the robot. Apart from the longitude heuristic, the optimal object order should also obey the acyclic dependency graph of the goal arrangement. The dependency graph is created by checking if the goal region of each object o_i prevents other objects from being placed at their goal regions, if so, there will be edges going from the objects that are blocked by o_i like the right image of Fig. 2 (b) illustrates. Object o_i should not be placed at its goal region when there are still edges points to it. The final object stage topology is generated by performing the topological sort on the dependency graph while respecting the longitude heuristic for objects that are not dependent on each other.

C. Single-Stage MCTS planner

Our Single-Stage MCTS (SS-MCTS) planner aims to move one specific object o_k from its current region $a^t[o_k]$ to the goal $a^g[o_k]$. In other words, the search halts when the objective $a^{t'}[o_k] = a^g[o_k]$ is achieved at some step $t' \geq t$. To better present our ideas, we introduce several new notations as follows. Assume we are now in the SS-MCTS planner that focuses on the k -th object o_k in the generated topology, and the current step count is t . All the objects that have been relocated to their goal regions form a set of static objects $\mathcal{O}_s = \{o_1, \dots, o_{k-1}\}$ and the rest are represented as $\mathcal{O}_r = \{o_k, \dots, o_n\}$. In the SS-MCTS focusing on object o_k , only the objects in \mathcal{O}_r are subject to be relocated.

The current arrangement a^t and the goal arrangement a^g contain the most up-to-date pairwise corresponded elements denoting objects' current/goal regions. Inside the tree, the parent and child tree nodes are linked by robot action r^t that relocates a single object o_i in \mathcal{O}_r from region p_i^t to p_i^{t+1} , forming a new arrangement a^{t+1} . The associated reward function value is assigned as the negation of the Euclidean distance between two regions, i.e., $-\|p_k^t - p_k^{t+1}\|_2$. The following paragraphs reveal the details of our SS-MCTS by fitting them into the standard MCTS paradigm.

Selection: The SS-MCTS planner balances the exploration and exploitation by utilizing the tuned Upper Confidence Bound (UCB) [24]. In the selection process, we pick a leaf node by going through successive child nodes maximizing the UCB values starting from the root. If the selected leaf node has already been visited, the expansion module introduced below is applied to further grow the tree.

Algorithm 1: new_region

Data: $o_i, o_k, \{o_d\}, a^t, a^g$

Result: $P_i^r = \{p_i^1, \dots, p_i^m\}$

```

1  $P_i^r = \emptyset$ 
2  $V(\pi(r_{pick})) = \text{LMP}(a^t[o_k])$ 
3  $V(\pi(r_{place})) = \text{LMP}(a^g[o_k])$ 
4  $\{V(\pi(r_{pick}^d))\} = \text{LMP}(a^t[\{o_d\}])$ 
5 for region candidates  $p_i \in P$  do
6   if collision_free( $p_i, \{a^t \setminus a^t[o_i], \{V(\pi(r_{pick}^d))\},$ 
7      $V(\pi(r_{pick})), V(\pi(r_{place}))\}$ )
8     then
9        $V(\pi(r_{place}^i)) = \text{LMP}(p_i)$ 
10      if collision_free( $V(\pi(r_{place}^i)), a^t \setminus a^t[o_i]$ ) then
11         $P_i^r.add(p_i)$ 
12        if size( $P_i^r$ ) =  $m$  then
13          break
13 return  $P_i^r$ 

```

Expansion: We present an efficient subgoal-focused expansion algorithm that shrinks the search space, which in result leads to a higher chance of finding valid solutions. The objective of the SS-MCTS is carried over to be the subgoal of the expansion module, i.e., relocating object of interest o_k to its goal region, and the tree expands focusing on it. In order to achieve the subgoal, first, the planner finds all objects O_b currently prevent o_k from being relocated to its goal region using a function called get_blocking_objects() (line 1 of Algorithm 2). It starts from calculating the picking and placing tunnel based on the current and goal region of o_k . All remaining objects except o_k should be moved to other regions if they are currently inside the two tunnels. In addition, because o_k becomes a static object in the following SS-MCTS focusing on other objects, the planner needs to ensure the remaining objects can still be accessed after placing o_k at its goal region. Thus, objects whose picking tunnel intersects with o_k placed at its goal region are added to the blocking object list O_b as well.

Algorithm 2: Expansion

Data: TreeNode $T_p(o_k, a^t, a^g, O_r)$

Result: TreeNode $T_c(o_k, a^{t+1}, a^g, O_r)$

```

1  $O_b = \text{get\_blocking\_objects}(o_k, a^t, a^g, O_r)$ 
2 if  $O_b \neq \emptyset$  then
3   while True do
4      $O'_b = \emptyset$ 
5     for  $o_i \in O_b$  do
6        $V(\pi(r_{pick}^i)) = \text{LMP}(a^t[o_i])$ 
7        $O_b^{ip} = \text{collision\_objs}(O_r \setminus o_i, V(\pi(r_{pick}^i)))$ 
8       if  $O_b^{ip} = \emptyset$  then
9          $V(\pi(r_{place}^i)) = \text{LMP}(a^g[o_i])$ 
10         $O_b^{id} = \text{collision\_objs}(O_r \setminus o_i, V(\pi(r_{place}^i)))$ 
11        if  $O_b^{id} = \emptyset$  and Valid( $a^g[o_i], o_k$ ) then
12           $T_p.add\_child(T_c(a^{t+1}[o_i] = a^g[o_i]))$ 
13        else
14          for  $k \leftarrow i-1$  to 1 do
15             $P_i^r = \text{new\_region}(o_i, o_k, o_{\{1\dots k\}}, a^t, a^g)$ 
16            if  $P_i^r$  then
17              for  $p_i^r \in P_i^r$  do
18                 $T_p.add\_child(T_c(a^{t+1}[o_i] = p_i^r))$ 
19              break
20        else
21          for  $o_j \in O_b^{ip}$  do
22             $V(\pi(r_{pick}^j)) = \text{LMP}(a^t[o_j])$ 
23            if collision_free( $O_r \setminus o_j, V(\pi(r_{pick}^j))$ ) then
24              for  $k \leftarrow j-1$  to 1 do
25                 $P_j^r = \text{new\_region}(o_j, o_k, o_{\{1\dots k, i\}}, a^t, a^g)$ 
26                if  $P_j^r$  then
27                  for  $p_j^r \in P_j^r$  do
28                     $T_p.add\_child(T_c(a^{t+1}[o_j] = p_j^r))$ 
29                  break
30                else
31                   $O'_b.add(o_j)$ 
32            halting\_condition()
33        else
34           $T_p.add\_child(T_c(a^{t+1}[o_k] = a^g[o_k]))$ 
35 return  $T_p.child[0]$ 

```

Next, we propose Algorithm 1 to generate new valid region candidates for the objects $o_i \in O_b$. A helper function called collision_free() detects whether there is a collision between the inputs. Each valid region candidate p_i for object o_i should not collide with the following elements: 1. all the regions currently occupied by other objects $a^t \setminus a^t[o_i]$. 2. the picking and placing tunnel regarding object of interest o_k . 3. the picking tunnels of a dependency objects set $\{o_d\}$ (line 6). The dependency objects are those who need to be relocated to fulfill the subgoal but it is currently being blocked by o_i . 4. Finally, all region candidates that meet

the abovementioned constraints form the final list of valid regions P_i^r if their corresponding relocation tunnels are feasible (line 9). During the actual execution, we sort the potential region candidates P by the increasing distance to o_i so that it better aligns with the reward function. In addition, an upper tree expansion threshold is set to prevent the tree from growing too wide while still maintaining decent performance.

The complete expansion algorithm is shown in Algorithm 2 with the aid of additional helper functions. The `collision_objs()` function (line 7, 10) takes a list of objects and a robot motion tunnel as inputs and returns all objects in the list that collide with the input tunnel. Also, the notation O_b^{ip} and O_b^{id} denote all objects that block the picking and placing tunnels of object o_i , respectively. The algorithm starts at parent tree node T_p by checking if both the picking and placing tunnels for the object of interest o_k are collision-free, if so, only one child tree node T_c that puts o_k directly to its goal region is created, which means the subgoal is achieved (line 1, 2, 34). Otherwise, the subgoal-blocking objects $o_i \in O_b$ are further divided into the following three categories where different strategies are applied: 1. The o_i will be directly placed at its final goal region $a^g[o_i]$ if the corresponding robot motion is collision-free and the goal region does not overlap with the tunnels of o_k (line 12). 2. If only the picking tunnel for o_i is available, valid regions that do not block the picking tunnel for objects earlier in the topology are proposed using Algorithm 1 and added to the tree (line 14-19). 3. If even the picking tunnel for o_i is not available, the algorithm first finds all objects O_b^{ip} blocking it. For each object $o_j \in O_b^{ip}$ that can be accessed, new regions are proposed with an additional dependency object setting as o_i so that the picking tunnel of o_i can be cleared (line 21-29). On the other hand, objects that are not accessible will be added to O_b' as the focus of the next iteration (line 31). In the `halting_condition()` function, the expansion process stops if new tree nodes are created, otherwise, the subgoal-blocking object set O_b will be replaced by O_b' and the expansion enters the next round. However, if the search depth reaches a certain threshold without making progress, O_b is changed to all the feasible objects, aiming to guide the search out of the stuck node. Finally, the expansion algorithm returns the first child node found during the process, from where the simulation starts (line 35). The high-level ideology of our expansion algorithm is that it grows the tree by hierarchically moving blocking objects out of the picking and placing tunnels for object of interest o_k . Eventually, both tunnels of o_k become collision-free, and our subgoal is fulfilled. Furthermore, our method can handle complex non-monotone problems mentioned in work [33] where o_k must be relocated to a buffer region before others because $o_j \in O_b^{ip}$ can potentially be set as o_k during the search process (line 21).

Simulation: This part follows the standard MCTS pipeline [24]. A rollout process grows a pathological tree from the chosen node in the selection or expansion module

until the object of interest o_k is relocated to its goal region. During the process, the relocation region for the object is randomly selected from the result returned by Algorithm 1.

Back-propagation: The reward function is set to be the negation of the accumulated region displacement distances when the simulation ends, as it is the term we seek to minimize. All tree nodes from the leaf where the simulation starts until the root receive the reward and one visited count during the backpropagation process.

The SS-MCTS planner halts when the current tree node achieves the objective. The sub-plan $\{r^t, \dots, r^{t+q}\}$ can be recovered by backward tree traversal.

D. Multi-Stage MCTS planner

The MS-MCTS planner comprises n ordered SS-MCTS. The SS-MCTS at index i sets its object of interest as o_i from the generated object stage topology introduced above. By extracting and combining all the sub-plans from the SS-MCTS planners, we get the initial global plan $R' = \{(r_{pick}^0, r_{place}^0), (r_{pick}^1, r_{place}^1), \dots\}$ that moves all objects from the start arrangement a^s to the goal arrangement a^g . The goal plan R' then goes through two optimization steps. In the first step, continuous action segments involving the same object $\{(r_{pick}^t, r_{place}^t), \dots, (r_{pick}^{t+k}, r_{place}^{t+k})\}$ will be combined to one single action $\{(r_{pick}^t, r_{place}^{t+k})\}$. The second step checks all non-adjacent action pairs (r^t, r^{t+k}) concerning the same object and changes it to $(r^t = (r_{pick}^t, r_{place}^{t+k}))$ if the actions in between $\{r^t, \dots, r^{t+k}\}$ can be still be performed without collision. These two optimization steps shrink the length of the original plan and result in the final global plan R .

V. EXPERIMENTS

A. Simulation Result

We create randomly generated start and goal arrangements of five increasing difficulty levels to examine the performance of our MS-MCTS. The environment has a dimension of 20 by 20 units with 4-8 objects inside. All objects are presented by circles with a radius 1 unit and they are placed with a minimal distance of 4 units between the centers to leave some grasping space for the gripper. The picking and placing tunnel width is set to be 4 units. The 4 objects cases are considered to be easy, 5-6 to be medium, and 7-8 to be hard. For each difficulty level, 80 cases are generated to understand the method's performance comprehensively. Aside from our MS-MCTS, two additional non-monotone planner baselines, BiRRT(mRS) [9] and PERTS(CIRS) [2], are implemented to compare against our method. BiRRT(mRS) follows the BiRRT algorithm with tree nodes denoting different arrangements. The mRS monotone solver connects different tree nodes and finally forms the complete plan. PERTS(CIRS) divides the hard non-monotone case into a sequence of monotone cases. It utilizes perturbations to find valid buffer regions when the tree cannot grow further with the CIRS monotone solver. We use the following metrics for quantitative evaluation:

Task planner	Easy & Medium cases			Hard cases		
	Success rate (%) \uparrow	Number of steps \downarrow	Displacement distance \downarrow	Success rate (%) \uparrow	Number of steps \downarrow	Displacement distance \downarrow
BiRRT(mRS)	96	17.85 ± 9.53	166.25 ± 85.4	3	28.0 ± 9.9	270.92 ± 74.95
PERTS(CIRS)	83	31.53 ± 42.13	280.23 ± 365.25	46	60.08 ± 46.65	507.71 ± 360.2
MS-MCTS (ours)	100	7.99 ± 2.38	61.5 ± 19.3	98	14.54 ± 2.47	105.8 ± 18.59

TABLE I: Experiments results reflect that our MS-MCTS outperforms the baseline methods in all metrics.

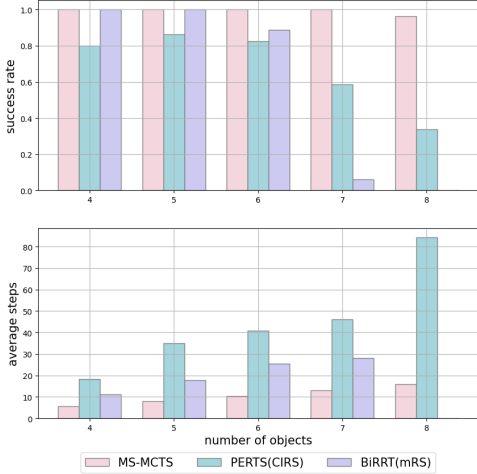


Fig. 3: Our MS-MCTS method has higher success rates and fewer steps than the baselines across all difficulty levels.

- **Success rate:** The percentage of successfully solved instances. Cases that are not solved within 30 seconds are considered as failures.
- **Number of steps:** The number of steps performed to achieve the goal arrangement.
- **Displacement distance:** The sum of displacement distance of all objects. The displacement distance is the Euclidean distance between the start and end regions.

Table I lists the test results. The last two metrics are presented by taking the average among all successful cases. We separate the difficulty levels to better showcase the strong performance of our method. Detailed visual comparisons of the success rate and the number of steps are shown in Fig. 3. Our MS-MCTS not only outperforms the baselines in all metrics but also stays stable within the same difficulty level, which can be seen from the relatively small standard deviation. In addition, the increasing difficulty levels have less effect on our method than others as the relocation distance grows almost linearly at a low rate. At the same time, the performance of the baselines drops significantly with respect to the increasing difficulty levels. In the most challenging settings, our MS-MCTS has a success rate that is three times as high as the best baseline PERTS(CIRS) while still maintaining an average step count that is 17% of it. The high success rate of our approach results from the better scalability of the multi-stage formulation as the search time consumption in our method grows linearly with the increasing number of objects.

B. Real Robot Experiments

We deploy our MS-MCTS method on a UR5e robot arm manipulator equipped with a Robotiq 2F-85 gripper to solve various rearrangement planning problems in a confined environment with dimensions of (140 cm, 70 cm, 38 cm). To better observe the robot motion from a top-down view, the testing space is constructed on a table surrounded by cardboard blocks on the three sides and a transparent "ceiling". The front end of the ceiling is represented by a string attached to the top of both sides. This leaves one opening at the front for the robot to access the objects inside. The objects in the scene are cylindrical tubes with colored coating to help distinguish between them.

We set up four real-world scenarios of two medium and two hard configurations with structured patterns in goal arrangements. The medium cases contain an average of 5 objects, while the hard ones have an average of 8.5 objects. Our MS-MCTS planner takes a^s, a^g as inputs, figures out the plan, and sends it to the robot arm manipulator for execution. The results reveal that our planner succeeded in finding valid plans for all test scenarios. In the medium cases, the average number of steps is 8.5, and the average displacement distance is 6.79 m. While for the hard instances, the average number of steps is 16.5, and the average displacement distance is 13.07 m. Fig. 1 shows a successfully performed medium level four objects flipping case. We can easily observe that the planner only generates the necessary moves to fulfill the goal arrangement. Also, the objects are relocated to the nearest buffer regions to minimize the total displacement distance. The experiments of other scenarios are available in our supplementary videos.

VI. CONCLUSION

This paper presents our Multi-Stage MCTS algorithm that solves non-monotone object rearrangement planning tasks in narrow, confined spaces. Our method decouples the generally considered NP-hard problems into a sequence of ordered stages, with each one focusing only on a specific object, which reduces the search space by a considerable amount. During relocation actions, the use of a linear motion planner minimizes the swept volume in the limited space and further leads to a higher chance of finding valid solutions. We fit the problem into the MCTS paradigm with customized designed functions to achieve high-quality results. The performance of our method is verified on various simulation cases with diverse difficulty levels and on the real robot. For future works, we seek to extend the planner into the 3D space with unknown, arbitrary objects to make it even more practical for real-world deployment.

REFERENCES

- [1] J. Reif and M. Sharir, "Motion planning in the presence of moving obstacles," *Journal of the ACM (JACM)*, vol. 41, no. 4, pp. 764–790, 1994.
- [2] R. Wang, Y. Miao, and K. E. Bekris, "Efficient and high-quality prehensile rearrangement in cluttered and confined spaces," in *2022 International Conference on Robotics and Automation (ICRA)*. IEEE, 2022, pp. 1968–1975.
- [3] P. C. Chen and Y. K. Hwang, "Practical path planning among movable obstacles," Sandia National Labs., Albuquerque, NM (USA), Tech. Rep., 1990.
- [4] M. Stilman and J. J. Kuffner, "Navigation among movable obstacles: Real-time reasoning in complex environments," *International Journal of Humanoid Robotics*, vol. 2, no. 04, pp. 479–503, 2005.
- [5] C. R. Garrett, R. Chitnis, R. Holladay, B. Kim, T. Silver, L. P. Kaelbling, and T. Lozano-Pérez, "Integrated task and motion planning," *Annual review of control, robotics, and autonomous systems*, vol. 4, pp. 265–293, 2021.
- [6] S. Srivastava, E. Fang, L. Riano, R. Chitnis, S. Russell, and P. Abbeel, "Combined task and motion planning through an extensible planner-independent interface layer," in *2014 IEEE international conference on robotics and automation (ICRA)*. IEEE, 2014, pp. 639–646.
- [7] M. Stilman, K. Nishiwaki, S. Kagami, and J. J. Kuffner, "Planning and executing navigation among movable obstacles," *Advanced Robotics*, vol. 21, no. 14, pp. 1617–1634, 2007.
- [8] M. Stilman and J. Kuffner, "Planning among movable obstacles with artificial constraints," *The International Journal of Robotics Research*, vol. 27, no. 11-12, pp. 1295–1307, 2008.
- [9] M. Stilman, J.-U. Schamburek, J. Kuffner, and T. Asfour, "Manipulation planning among movable obstacles," in *Proceedings 2007 IEEE international conference on robotics and automation*. IEEE, 2007, pp. 3327–3332.
- [10] A. Krontiris and K. E. Bekris, "Efficiently solving general rearrangement tasks: A fast extension primitive for an incremental sampling-based planner," in *2016 IEEE International Conference on Robotics and Automation (ICRA)*. IEEE, 2016, pp. 3924–3931.
- [11] G. Havur, G. Ozbilgin, E. Erdem, and V. Patoglu, "Geometric rearrangement of multiple movable objects on cluttered surfaces: A hybrid reasoning approach," in *2014 IEEE International Conference on Robotics and Automation (ICRA)*. IEEE, 2014, pp. 445–452.
- [12] K. Gao, D. Lau, B. Huang, K. E. Bekris, and J. Yu, "Fast high-quality tabletop rearrangement in bounded workspace," in *2022 International Conference on Robotics and Automation (ICRA)*. IEEE, 2022, pp. 1961–1967.
- [13] W. Liu, C. Paxton, T. Hermans, and D. Fox, "Structformer: Learning spatial structure for language-guided semantic rearrangement of novel objects," in *2022 International Conference on Robotics and Automation (ICRA)*. IEEE, 2022, pp. 6322–6329.
- [14] A. Curtis, X. Fang, L. P. Kaelbling, T. Lozano-Pérez, and C. R. Garrett, "Long-horizon manipulation of unknown objects via task and motion planning with estimated affordances," in *2022 International Conference on Robotics and Automation (ICRA)*. IEEE, 2022, pp. 1940–1946.
- [15] W. Goodwin, S. Vaze, I. Havoutis, and I. Posner, "Semantically grounded object matching for robust robotic scene rearrangement," in *2022 International Conference on Robotics and Automation (ICRA)*. IEEE, 2022, pp. 11 138–11 144.
- [16] A. H. Qureshi, A. Mousavian, C. Paxton, M. C. Yip, and D. Fox, "Nerp: Neural rearrangement planning for unknown objects," *arXiv preprint arXiv:2106.01352*, 2021.
- [17] A. Zeng, P. Florence, J. Tompson, S. Welker, J. Chien, M. Attarian, T. Armstrong, I. Krasin, D. Duong, V. Sindhwani, *et al.*, "Transporter networks: Rearranging the visual world for robotic manipulation," in *Conference on Robot Learning*. PMLR, 2021, pp. 726–747.
- [18] W. Yuan, K. Hang, D. Kragic, M. Y. Wang, and J. A. Stork, "End-to-end nonprehensile rearrangement with deep reinforcement learning and simulation-to-reality transfer," *Robotics and Autonomous Systems*, vol. 119, pp. 119–134, 2019.
- [19] W. Yuan, J. A. Stork, D. Kragic, M. Y. Wang, and K. Hang, "Rearrangement with nonprehensile manipulation using deep reinforcement learning," in *2018 IEEE International Conference on Robotics and Automation (ICRA)*. IEEE, 2018, pp. 270–277.
- [20] A. Goyal, A. Mousavian, C. Paxton, Y.-W. Chao, B. Okorn, J. Deng, and D. Fox, "Ifor: Iterative flow minimization for robotic object rearrangement," in *Proceedings of the IEEE/CVF Conference on Computer Vision and Pattern Recognition*, 2022, pp. 14 787–14 797.
- [21] R. Wang, K. Gao, D. Nakhimovich, J. Yu, and K. E. Bekris, "Uniform object rearrangement: From complete monotone primitives to efficient non-monotone informed search," in *2021 IEEE International Conference on Robotics and Automation (ICRA)*. IEEE, 2021, pp. 6621–6627.
- [22] R. Wang, K. Gao, J. Yu, and K. Bekris, "Lazy rearrangement planning in confined spaces," in *Proceedings of the International Conference on Automated Planning and Scheduling*, vol. 32, 2022, pp. 385–393.
- [23] J. Lee, C. Nam, J. Park, and C. Kim, "Tree search-based task and motion planning with prehensile and non-prehensile manipulation for obstacle rearrangement in clutter," in *2021 IEEE International Conference on Robotics and Automation (ICRA)*. IEEE, 2021, pp. 8516–8522.
- [24] C. B. Browne, E. Powley, D. Whitehouse, S. M. Lucas, P. I. Cowling, P. Rohlfshagen, S. Tavener, D. Perez, S. Samothrakis, and S. Colton, "A survey of monte carlo tree search methods," *IEEE Transactions on Computational Intelligence and AI in games*, vol. 4, no. 1, pp. 1–43, 2012.
- [25] D. Silver, T. Hubert, J. Schrittwieser, I. Antonoglou, M. Lai, A. Guez, M. Lanctot, L. Sifre, D. Kumaran, T. Graepel, *et al.*, "A general reinforcement learning algorithm that masters chess, shogi, and go through self-play," *Science*, vol. 362, no. 6419, pp. 1140–1144, 2018.
- [26] M. C. Fu, "Alphago and monte carlo tree search: the simulation optimization perspective," in *2016 Winter Simulation Conference (WSC)*. IEEE, 2016, pp. 659–670.
- [27] T. M. Moerland, J. Broekens, A. Plaat, and C. M. Jonker, "A0c: Alpha zero in continuous action space," *arXiv preprint arXiv:1805.09613*, 2018.
- [28] Y. Labbé, S. Zagoruyko, I. Kalevatykh, I. Laptev, J. Carpentier, M. Aubry, and J. Sivic, "Monte-carlo tree search for efficient visually guided rearrangement planning," *IEEE Robotics and Automation Letters*, vol. 5, no. 2, pp. 3715–3722, 2020.
- [29] H. Song, J. A. Hausteine, W. Yuan, K. Hang, M. Y. Wang, D. Kragic, and J. A. Stork, "Multi-object rearrangement with monte carlo tree search: A case study on planar nonprehensile sorting," in *2020 IEEE/RSJ International Conference on Intelligent Robots and Systems (IROS)*. IEEE, 2020, pp. 9433–9440.
- [30] J. E. King, V. Ranganeni, and S. S. Srinivasa, "Unobservable monte carlo planning for nonprehensile rearrangement tasks," in *2017 IEEE International Conference on Robotics and Automation (ICRA)*. IEEE, 2017, pp. 4681–4688.
- [31] S. K. Chan, "An iterative general inverse kinematics solution with variable damping," Ph.D. dissertation, University of British Columbia, 1987.
- [32] J. Huynh, "Separating axis theorem for oriented bounding boxes," URL: [jkh.me/files/tutorials/Separating% 20Axis% 20Theorem% 20for% 20Oriented% 20Bounding% 20Boxes. pdf](http://jkh.me/files/tutorials/Separating%20Axis%20Theorem%20for%20Oriented%20Bounding%20Boxes.pdf), 2009.
- [33] A. Krontiris and K. E. Bekris, "Dealing with difficult instances of object rearrangement," in *Robotics: Science and Systems*, vol. 1123, 2015.